European Heart Journal (2008) **29**, 2234–2243
doi:10.1093/eurheartj/ehn329

Electrical remodelling of the left and right atria due to rheumatic mitral stenosis†

Bobby John[1,2], Martin K. Stiles[1], Pawel Kuklik[1], Sunil T. Chandy[2], Glenn D. Young[1], Lorraine Mackenzie[1], Lukasz Szumowski[3], George Joseph[2], Jacob Jose[2], Stephen G. Worthley[1], Jonathan M. Kalman[4], and Prashanthan Sanders[1]*

[1]Cardiovascular Research Center, Department of Cardiology, Royal Adelaide Hospital and the Disciplines of Medicine and Physiology, University of Adelaide, Adelaide, Australia; [2]Department of Cardiology, Christian Medical College, Vellore, India; [3]Institute of Cardiology, Warsaw, Poland; and [4]Department of Cardiology, Royal Melbourne Hospital and Department of Medicine, University of Melbourne, Victoria, Australia

Received 21 December 2007; revised 17 June 2008; accepted 19 June 2008; online publish-ahead-of-print 10 July 2008

Aims To characterize the atrial remodelling in mitral stenosis (MS).

Methods and results Twenty-four patients with severe MS undergoing commissurotomy and 24 controls were studied. Electrophysiological evaluation was performed in 12 patients in each group by positioning multi-electrode catheters in both atria to determine the following: effective refractory period (ERP) at 10 sites at 600 and 450 ms; conduction time; conduction delay at the crista terminalis (CT); and vulnerability for atrial fibrillation (AF). P-wave duration (PWD) was determined on the surface ECG. In the remaining 12 patients in each group, electroanatomic maps of both atria were created to determine conduction velocity and identify regions of low voltage and electrical silence. Patients with MS had larger left atria (LA) ($P < 0.0001$); prolonged PWD ($P = 0.0007$); prolonged ERP in both LA ($P < 0.0001$) and right atria (RA) ($P < 0.0001$); reduced conduction velocity in the LA ($P = 0.009$) and RA ($P < 0.0001$); greater number ($P < 0.0001$) and duration ($P < 0.0001$) of bipoles along the CT with delayed conduction; lower atrial voltage in the LA ($P < 0.0001$) and RA ($P < 0.0001$); and more frequent electrical scar ($P = 0.001$) compared with controls. Five of twelve with MS and none of the controls developed AF with extra-stimulus ($P = 0.02$).

Conclusion Atrial remodelling in MS is characterized by LA enlargement, loss of myocardium, and scarring associated with widespread and site-specific conduction abnormalities and no change or an increase in ERP. These abnormalities were associated with a heightened inducibility of AF.

Keywords Rheumatic mitral stenosis • Atrial remodelling • Atrial fibrillation

Introduction

Rheumatic heart disease (RHD) is a major health problem in developing countries and in some indigenous populations in developed countries.[1,2] It is estimated that at least 15.6 million people suffer from RHD worldwide.[2] In addition, there is evidence to suggest that the prevalence of this condition will continue to increase with ~2.4 million children aged 5–14 manifesting features of RHD.[2]

While in developed countries the common causes of atrial fibrillation (AF) are related to congestive heart failure, hypertension, and increasing age;[3] in the developing world, chronic RHD is one of the common forms of structural heart disease associated with AF, with over 40% of afflicted individuals developing AF.[4] The latter population is largely young and the onset of AF heralds significant morbidity with costs to the individual and society. In addition, it is well recognized that the risk for stroke due to AF in this population is increased to a greater extent (17.5-fold).[5]

Despite the profound consequences of AF in this population the electrophysiological mechanisms by which rheumatic mitral stenosis (MS) predisposes to the development of AF remain unknown. Chronic MS results in left atrial 'stretch' due to elevated pressure.

* Corresponding author. Tel: +61 8 8222 2723, Fax: +61 8 8222 2722, Email: prash.sanders@adelaide.edu.au

† Presented in part by Dr John and received Young Investigator Award at the 2nd Asia-Pacific AF Symposium, November 2006, Tokyo, Japan; and at the Heart Rhythm Society's 27th Annual Scientific Sessions, May 2006, Boston, USA and published in abstract form (Heart Rhythm 2006; 3: S194).

While left atrial enlargement *per se* may be sufficient to explain the increase in AF in this population, we hypothesized that chronic rheumatic MS also results in significant electrical remodelling, thereby creating the substrate for atrial arrhythmias.

Percutaneous balloon mitral commissurotomy (PBMC) is now the treatment of choice for patients with severe MS and favourable valve morphology. In patients referred for PBMC we aimed to characterize the electrophysiological and electroanatomical abnormalities within the right (RA) and left atria (LA) that occur as a result of rheumatic MS.

Methods

Study population

The study comprised 24 consecutive patients with rheumatic MS undergoing PBMC. The sample size was powered (power >0.9) to detect a 20% reduction ($\sim$0.5 mV) in mean voltage between disease and control samples based on previous study.[6] Patients were selected on the basis of having severe MS with a mitral valve area of <1.5 cm^2 with significant symptoms (NYHA class ≥ 2) and mitral valve morphology suitable for PBMC as determined by the Wilkins criteria (score <10). Patients were excluded if they had any suggestion of other structural heart disease (coronary artery disease or left ventricular dysfunction), hypertension, atrial arrhythmia, or had used amiodarone in the prior 6 months. A further 24 patients having radiofrequency ablation for left-sided accessory pathways without evidence of structural heart disease were studied as the control population. This group was selected from consecutive patients, within 10 years in age of an enrolled MS patient, referred for ablation and meeting the inclusion and exclusion criteria ensuring that the two samples were equally distributed within the different age ranges of 18–28, 28–38, 38–48, and 48–58 years. The technique utilized for PBMC has been detailed elsewhere.[7]

All patients gave written informed consent to the study, which was approved by each institutional Clinical Research and Ethics Committee. All anti-arrhythmic drugs, including calcium-channel blockers, were ceased at least 5 half-lives before the study. In addition, all patients with MS underwent transoesophageal echocardiography to exclude the presence of atrial thrombus. Twelve patients in each group underwent electrophysiological study and the remaining 12 in each group underwent electroanatomical mapping.

Electrophysiological study

Electrophysiological study was performed in the fasting state with sedation utilizing midazolam. Detailed electrophysiological evaluation of the RA and LA was performed before PBMC. The following catheters were positioned within the RA (*Figure 1*): (i) 10-pole catheter with 2-5-2 mm inter-electrode spacing (Daig Electrophysiology) in the coronary sinus (CS) with the proximal bipole positioned at the CS ostium as determined in the best septal left anterior oblique view; (ii) 20-pole catheter with 2-5-2 mm inter-electrode spacing (Daig Electrophysiology) placed along the lateral right atrium (LRA); (iii) 4-pole ablation catheter with 2-5-2 mm inter-electrode spacing (4 mm tip Celsius, Biosense-Webster) along the high-septal RA (SRA); and (iv) 20-pole 'crista' catheter with 1-3-1 mm inter-electrode

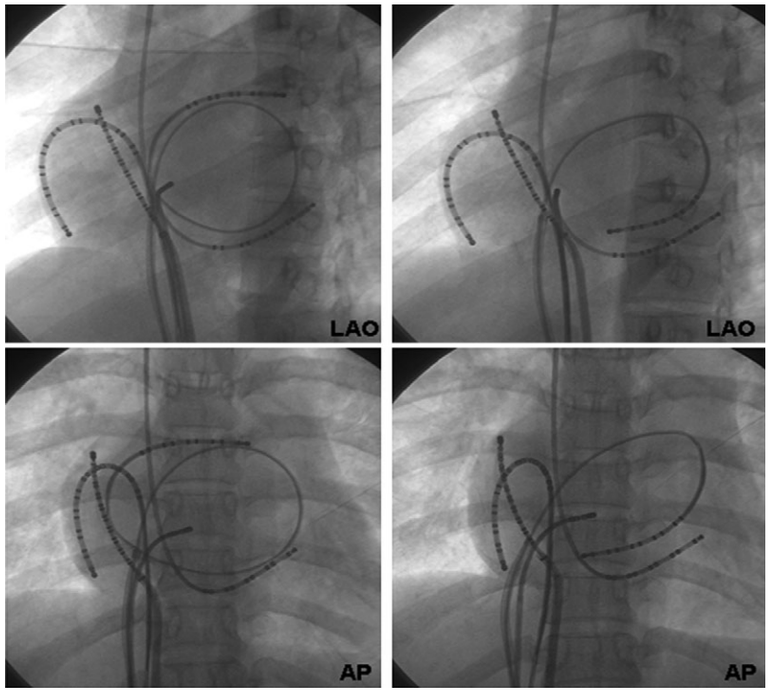

Figure 1 Fluoroscopic images demonstrating the catheter position for the study protocol. Each set of panels demonstrates the left anterior oblique (LAO) and anterior-posterior (AP) projections. The right sided catheters are positioned along the LRA, crista terminalis, His and the coronary sinus. A single 10-pole catheter in the LA is seen sequentially positioned at the LA-roof (left) and the inferior-LA along the posterior-mitral annulus (right).

spacing (Biosense-Webster) positioned with the aid of a long sheath along the crista terminalis (CT) and standardized such that the second bipole lay at the junction of the superior vena cava with the RA as determined by fluoroscopy and intracardiac echocardiography (ICE; Acunav, Siemens Medical). For LA mapping, a single 10-pole catheter with 2-5-2 mm inter-electrode spacing (Biosense-Webster) was inserted via trans-septal puncture. This catheter was stabilized with the use of a long sheath (Preface, Biosense-Webster) and sequentially positioned as follows along (*Figure 1*): (i) LA-roof; (ii) inferior-LA; (iii) mid-posterior-LA; and (iv) LA-appendage.

Surface ECG and bipolar endocardial electrograms were continuously monitored and stored on a computer-based digital amplifier/recorder system for offline analysis (Bard Electrophysiology). Intracardiac electrograms were filtered from 30 to 500 Hz, and measured with computer-assisted calipers at a sweep speed of 200 mm/s.

Effective refractoriness

Atrial effective refractory period (ERP) was evaluated at twice diastolic-threshold at cycle lengths (CL) of 600 and 450 ms using an 8-beat drive followed by an extra-stimulus (S_2), starting with an S_2 coupling interval of 150 ms increasing in 10 ms increments. ERP was defined as the longest coupling interval failing to propagate to the atrium. At each site the ERP was measured three times during each CL and averaged. If ERP varied by >10 ms an additional two measurements were made and the total number averaged. ERP was measured from the following sites: (i) distal-CS; (ii) proximal-CS; (iii) low-LRA; (iv) high-LRA; (v) high-SRA; (vi) LA-appendage; (vii) posterior-LA; (viii) RSPV-LA-roof junction; (ix) LSPV-LA-roof junction; and (x) inferior-LA. The heterogeneity of ERP was determined using the coefficient of variation (CoV = SD/mean $\times$ 100%).

Atrial conduction

Local conduction time was assessed along linearly placed catheters by pacing the distal bipole (1/2) and determining the conduction time to the proximal bipole (9/10) at the LA-roof, inferior-LA, CS, and LRA. Conduction time at each site was averaged over 10 beats during stable capture at CLs of 600 and 450 ms.

P-wave duration (PWD) was averaged over 10 beats as a surrogate marker of inter-atrial conduction time and measured on lead II of the surface ECG.

Site-specific conduction

Anatomically determined site-specific conduction delay at the CT was determined during the drive (at 600 and 450 ms) and the shortest coupled conducted extra-stimulus from each pacing site. Conduction delay at the CT was analysed on each recording bipole of the crista catheter and defined as the presence of discrete double potentials (DP) separated by an isoelectric interval or fractionated signals (FS) of $\geq$50 ms; both the number of bipoles demonstrating conduction delay and the maximum electrogram duration were evaluated.

Inducibility of atrial fibrillation

Atrial vulnerability to develop AF by single extra-stimulus was noted during ERP determination. AF was defined as irregular atrial activity lasting >30 s. AF lasting >5 min was considered sustained; when this occurred, no further data were acquired.

Electroanatomic mapping

Electroanatomic maps were created of both atria during sinus rhythm using the CARTO mapping system (Biosense-Webster). The electroanatomic mapping system has been previously described in detail; the accuracy of the sensor position has been previously validated and is 0.8 mm and 5°.[8] In brief, the system records the 12-lead ECG and bipolar electrograms filtered at 30–400 Hz from the mapping and reference catheters.

Endocardial contact during point acquisition was facilitated by fluoroscopy, the catheter icon on the CARTO system, and ICE. Points were acquired in the auto-freeze mode if the stability criteria in space ($\leq$6 mm) and local activation time (LAT; $\leq$5 ms) were met. Mapping was performed with an equal distribution of points using a fill-threshold of 15 mm. Editing of points was performed offline. LAT was manually annotated to the peak of the largest amplitude deflection on bipolar electrograms. In the presence of DPs, the LAT was annotated at the largest potential. If the bipolar electrogram displayed equivalent maximum positive and negative deflections, the maximum negative deflection on the simultaneously acquired unipolar electrogram was used to annotate the LAT. Points not conforming to the 12-lead ECG P-wave morphology or $<$75% of the maximum voltage of the preceding electrogram were excluded. Regional atrial bipolar voltage and conduction velocity were analysed as previously described and are detailed below.[6]

Voltage analysis

For the purposes of evaluating regional voltage differences, each atrium was segmented using previously validated offline software.[9] The RA was segmented as the high- and low-LRA, high- and low-posterior-RA, high- and low-SRA, and anterior RA. The LA was segmented as posterior-LA, LA-roof, anterior-LA, septal-LA, inferior-LA, and lateral-LA. For each region and each atrium the mean voltage was determined by averaging the bipolar voltage of the points within the given region.

For the purposes of the voltage map, electrically silent areas (scar) were defined as the absence of recordable activity or a bipolar voltage amplitude $\leq$0.05 mV (the noise level of the system) and low voltage areas as contiguous areas of bipolar voltage $\leq$0.5 mV. The voltage contribution of each point to the surface area of the atria was determined using previously validated offline software.[9]

Conduction velocity analysis

Isochronal activation maps (5 ms intervals) of the atria were created and regional conduction velocity determined in the direction of the wave-front propagation (least isochronal crowding).[9] The system determines the conduction velocity between two points by expressing the distance between the points as a function of the difference in LAT. For the purposes of evaluating regional conduction differences, each atrium was segmented as above.

The proportion of points demonstrating delayed conduction was determined using the following definitions: (i) FS—complex activity of $\geq$50 ms duration and (ii) DP—potentials separated by an isoelectric interval of $\geq$50 ms.

Statistical analysis

All variables are reported as mean $\pm$ SD and assessed for normality utilizing the Shapiro–Wilk test. Normally distributed data were compared using two-sided paired or unpaired Student's *t*-test. Data that were not normally distributed were compared using the Wilcoxon signed-rank or Rank-sum tests, for paired and unpaired data, respectively. Categorical variables are reported as number and percentage, and compared using the Fisher's exact test.

Group data were analysed using a linear mixed effects model with group and anatomical region and their interaction (group*region) modelled as fixed effects with age as a covariate. A random patient identifier effect was added to the model to account for the possible

inter-dependencies between repeated observations within a patient. The fit of the model to the data was sufficient such that additional random effects were not added. The model was assessed for normality assumption violation via investigation of residuals. If the residuals were not normally distributed, the model was run on transformed data (log or square root). The model was initially run with a group*region interaction term. If the interaction term was not significant the model was re-run without the interaction term and the group and region main effects were reported accordingly. If a significant group*region interaction was present, region-by-region independent two-sided *t*-tests with adjustment via the sequential rejective bonferoni method were performed to resolve the site-specific differences causing the significant interaction. Statistical significance was established at $P < 0.05$.

Results

Patient characteristics

The two groups were comparable in age and left ventricular function (*Table 1*). Patients with MS had a mitral valve area of 0.9 ± 0.1 cm^2 associated with a mitral valve gradient of 17.3 ± 7.0 mmHg. This was associated with significant LA enlargement ($P < 0.0001$) and increased LA pressure ($P < 0.0001$) compared with controls. In addition, these patients demonstrated higher pulmonary artery pressures ($P = 0.0002$) compared with controls.

Prolongation of atrial refractoriness

At all 10 sites in both atria and at each CL, ERP was prolonged in patients with MS compared with controls (*Figure 2*); at a CL of 600 ms ($P < 0.0001$) and at a CL of 450 ms ($P < 0.0001$). Group by region interaction using the mixed effects model was only observed for a CL of 450 ms. Further analysis revealed that at a CL of 450 ms there was significant prolongation of the ERP at the following sites: LAA (232 ± 14 vs. 196 ± 17 ms, $P < 0.0001$); LSPV-LA-roof junction (256 ± 37 vs. 217 ± 24 ms, $P = 0.007$); posterior-LA (252 ± 24 vs. 225 ± 27 ms, $P = 0.02$); inferior-LA (249 ± 19 vs. 222 ± 19 ms, $P = 0.002$); proximal-CS (238 ± 21 vs. 212 ± 20 ms, $P = 0.006$); low-LRA (209 ± 18 vs. 172 ± 13 ms, $P < 0.0001$); and high-LRA (209 ± 25 vs. 174 ± 19 ms, $P = 0.001$). The ERP at RSPV-LA-roof junction ($P = 0.3$), high-SRA ($P = 0.1$) and distal-CS ($P = 0.6$) were comparable to the control group. Overall, the prolongation of ERP in patients with MS was associated with no change in the heterogeneity of ERP (LA 8.5 ± 2.3 vs. $9.9 \pm 2.9\%$, $P = 0.2$; RA 11.1 ± 3.0 vs. $13.2 \pm 4.4\%$, $P = 0.2$) and with preservation of physiological rate-adaptation of ERP.

Prolongation of atrial conduction time

The atrial conduction time was significantly prolonged within the LA in patients with MS compared with controls at 600 ms ($P = 0.004$) and at 450 ms ($P = 0.006$); at the inferior-LA (at 600 ms, 47.9 ± 5.0 vs. 32.8 ± 8.6 ms, $P < 0.001$; and at 450 ms, 49.6 ± 6.0 vs. 33.3 ± 9.6 ms, $P < 0.001$). However, there was no significant difference in conduction time at the LA-roof (at 600 ms, 41.6 ± 11.9 vs. 36.0 ± 6.3 ms, $P = 0.2$; and at 450 ms, 41.7 ± 12.2 vs. 35.0 ± 6.5 ms, $P = 0.1$); within the CS (at 600 ms, 33.7 ± 12.1 vs. 33.9 ± 5.2 ms, $P = 0.9$; and at 450 ms, 34.8 ± 12.6 vs. 35.2 ± 4.8 ms, $P = 0.9$) or the LRA (at 600 ms, 38.1 ± 7.4 vs. 35.2 ± 4.7 ms, $P = 0.3$; and at 450 ms, 37.9 ± 7.4 vs. 36.4 ± 5.1 ms, $P = 0.6$).

The PWD was significantly prolonged in patients with MS compared with controls; 139.6 ± 22.4 vs. 107.8 ± 13.1 ms ($P = 0.0007$).

Table 1 Patient characteristics

	Mitral stenosis ($n = 24$)	Control ($n = 24$)	*P*-value
Age (years)	31.5 ± 8.6	35.4 ± 11.6	0.2
Left atrial size			
Longitudinal (mm)	56.2 ± 5.6	43.7 ± 4.7	<0.0001
Transverse (mm)	50.1 ± 3.9	31.5 ± 5.1	<0.0001
Volume (mL)[a]	77.8 ± 14.3	23.8 ± 6.8	<0.0001
Right atrial size			
Longitudinal (mm)	46.6 ± 2.6	41.3 ± 5.2	0.005
Transverse (mm)	26.7 ± 3.1	31.1 ± 3.1	0.004
Volume (mL)[a]	18.3 ± 8.9	21.8 ± 5.9	0.03
LV ejection fraction (%)	62.8 ± 9.4	65.3 ± 8.2	0.5
LV size (mm)			
LV end-diastolic diameter	40.5 ± 7.2	45.6 ± 6.7	0.03
LV end-systolic diameter	27.8 ± 5.1	28.5 ± 4.2	0.6
Pressures (mmHg)			
Left atrial	24.0 ± 7.6	7.0 ± 5.2	<0.0001
Pulmonary artery	39.3 ± 15.6	17.9 ± 8.7	0.0002

[a]Atrial volume calculated echocardiographically using the equation for a prolate ellipsoid: V (mL) = π D_1 D_2 L/ 6, where D_1 and D_2 are the minor axis (width) as measured in 2 views (apical 4 chamber and parasternal long axis) at the mid-cavity level and L is the major axis (length) of the atrium as measured in the apical 4-chamber view from the posterior atrium to the level of the mitral/tricuspid annulus. Since the RA dimensions in the parasternal long axis view was not feasible D_1 was considered equal to D_2.

Site-specific conduction abnormalities

Patients with MS demonstrated significantly greater conduction abnormalities along the CT compared with controls; with a greater number of bipoles demonstrating DP/FS (at 600 ms, $P < 0.0001$ and with S_2 $P < 0.0001$; at 450 ms, $P < 0.0001$ and with S_2 $P < 0.0001$) and longer electrogram duration (at 600 ms, $P < 0.0001$ and with S_2 $P = 0.001$; at 450 ms, $P < 0.0001$ and with S_2 $P < 0.0001$) compared with controls (*Figure 3*). These abnormalities were observed both during constant pacing and increased further with extra-stimulus; at 600 ms and at 450 ms for number and duration ($P < 0.0001$). These data highlight the functional nature of the conduction delay at the CT evidenced by the variation of the extent of conduction abnormalities by rate and site of stimulation.

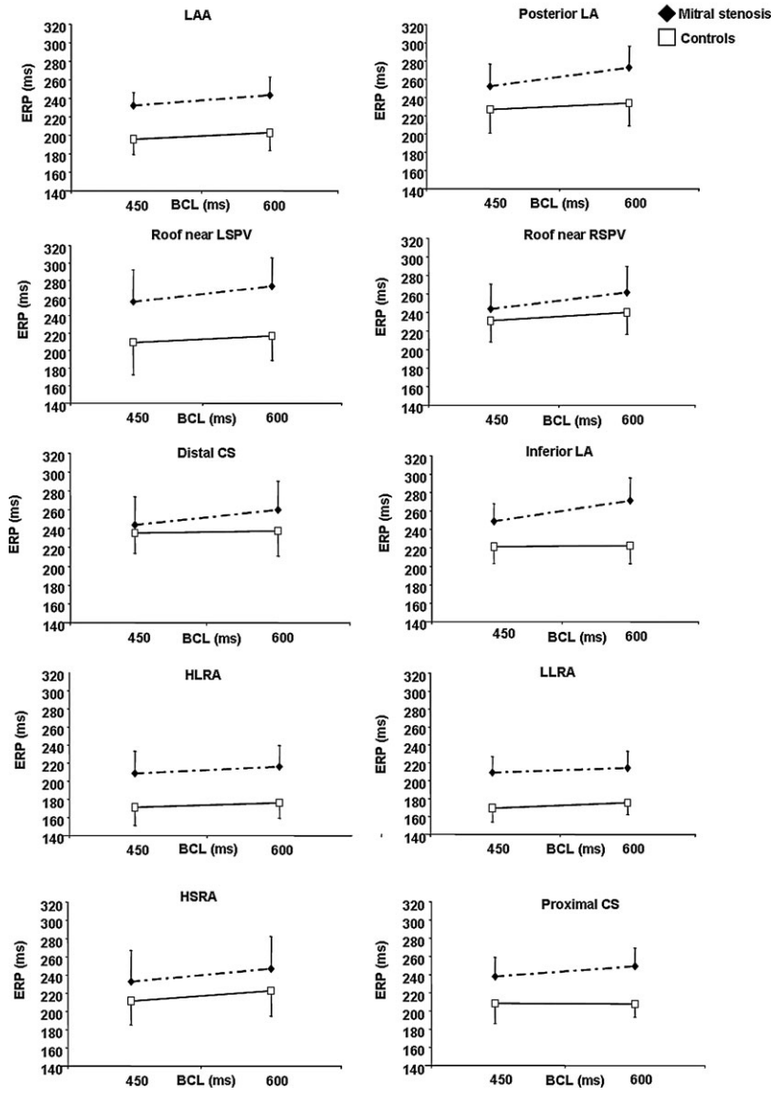

Figure 2 Effective refractory period at cycle lengths of 600 and 450 ms in patients with mitral stenosis and controls at each of the 10 sites evaluated. At each site and at each cycle length the effective refractory period was prolonged in patients with mitral stenosis compared with controls. Mixed effect group *P*-value for cycle lengths of 600 ($P < 0.0001$) and 450 ($P < 0.0001$). Group by region interaction was significant at cycle length of 450 ms for LAA, LSPV, posterior-LA, inferior-LA, proximal-CS, low-lateral-RA, high-lateral-RA. See text for details.

Vulnerability for atrial fibrillation

Patients with MS developed AF more frequently during electrophysiological study than controls: 5/12 vs. 0/12 ($P = 0.02$). In three of these patients, AF became sustained requiring cardioversion.

Electroanatomic mapping

A total of 231 $\pm$ 56 points/patient were analysed in the LA and RA using electroanatomical mapping.

Structural and voltage abnormalities

The LA volume was significantly greater in patients with MS compared with controls; 136 $\pm$ 46 vs. 86 $\pm$ 29 mL, respectively ($P = 0.005$). In contrast, there was no difference in the RA volume; 74 $\pm$ 23 vs. 69 $\pm$ 12 mL, respectively ($P = 0.5$). Indeed, in patients with MS, the marked enlargement of the LA resulted in significant compression of the RA as demonstrated in *Figure 4A*.

The mean bipolar voltage was reduced in both the LA and RA of patients with MS compared with controls; LA 1.8 $\pm$ 0.6 vs. 3.6 $\pm$ 0.6 mV ($P < 0.0001$) and RA 1.9 $\pm$ 0.6 vs. 3.3 $\pm$ 0.5 mV ($P < 0.0001$; *Figure 4B*), respectively. This decrease in voltage persisted in each region evaluated in the LA ($P < 0.0001$) and RA ($P < 0.0001$; *Figure 5*). Both atria in patients with MS demonstrated a greater percentage of the area below 1.5 mV than controls; this was observed to a greater extent in the LA

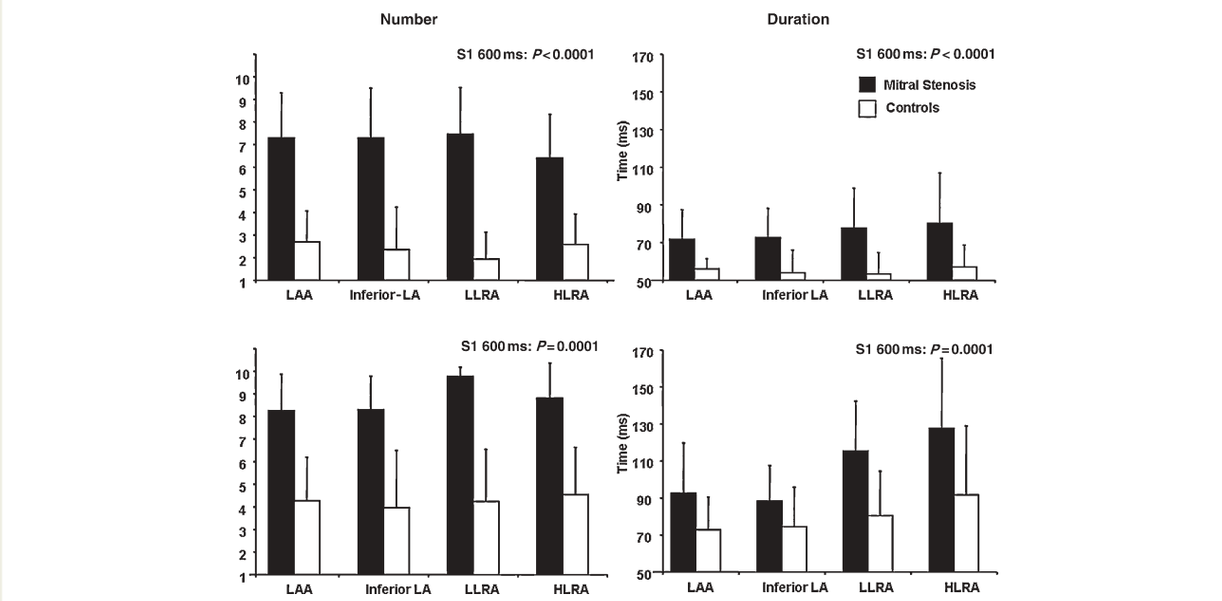

Figure 3 Number (left) and duration (right) of double potentials or fractionated electrograms along the crista terminalis during constant pacing at a cycle length of 600 ms (S1) and with the earliest captured extra-stimulus (S2). The information presented is from pacing sites at the LA-appendage (LAA), inferior-LA, low-lateral-RA (LLRA) and the high-lateral-RA (HLRA). Mixed effect group *P*-value for number and duration of DP with S1 and S2 at a cycle length of 600 is shown.

(44 vs. 22% $P = 0.0009$) than in the RA (38 vs. 30%, $P = 0.2$). In addition, 8 of the 12 patients with MS (67%) compared with none of the controls had regions of electrical silence ($P = 0.001$). Areas of electrical silence in the LA were localized to the posterior wall adjacent to the pulmonary veins (PVs) in 3, anterior-LA in 3, and septal-LA in 1; while in the RA it was localized to the LRA.

Abnormalities in conduction velocity

The total atrial activation time was significantly prolonged in patients with MS compared with controls (180 ± 36 vs. 154 ± 18 ms, respectively; $P = 0.04$). This was associated with significantly slower conduction in patients with MS compared with controls in both the LA (1.3 ± 0.3 vs. 1.7 ± 0.4 mm/ms, respectively; $P = 0.008$) and RA (1.0 ± 0.1 vs. 1.6 ± 0.3 mm/ms, respectively; $P < 0.0001$). Slower conduction velocity persisted in all regions in both the LA ($P = 0.009$) and RA ($P < 0.0001$) in patients with MS compared with controls (*Figure 6*).

Patients with MS demonstrated a significantly greater number of points with DP or FS than controls: in the LA this represented 30 ± 10 vs. 13 ± 9% of points, respectively ($P = 0.0005$) and in the RA this represented 46 ± 24 vs. 10 ± 9% of points, respectively ($P < 0.0001$). These points with DP or FS were distributed throughout the atria with a clustering along the CT in the RA and the anterior wall and roof in the LA. This clustering was consistent with regions of site-specific conduction abnormalities such as the CT or in proximity/association with regions of low voltage and scarring.

Discussion

Major findings

This study presents new information on the nature of the electrophysiological and electroanatomical abnormalities within the atria in patients with rheumatic MS. It provides unique characterization of the abnormalities within both the LA and RA compared with controls.

First, it demonstrates structural abnormalities characterized by left atrial dilatation and areas of low voltage and electrical silence suggesting the loss of atrial myocardium.

Second, this was associated with conduction abnormalities within the atria characterized by regions of DPs, fractionated electrograms, prolonged conduction times and PWD, and site-specific conduction delay.

Third, patients with MS demonstrated no change or an increase in ERP, which is consistent with prior studies evaluating clinical substrates for AF but in contrast to the remodelling attributed to AF itself.

Fourth, potentially as a consequence of these abnormalities, patients with MS were more susceptible to develop AF.

Importantly, while these abnormalities were observed within both atria, their extent was greater in the LA than the RA. Thus, the present study suggests that the substrate for AF in patients with MS is related to the structural abnormalities and the associated widespread and site-specific conduction abnormalities.

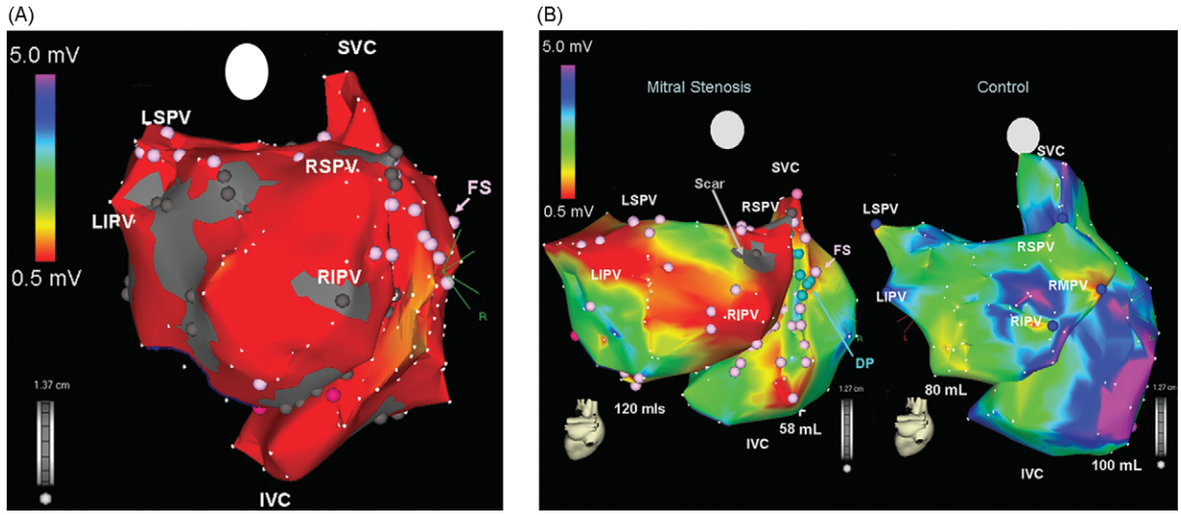

Figure 4 (*A*) Electroanatomic map of a patient with MS. Shown is the posterior-anterior projections of both atria. Note the markedly enlarged LA (172 mL) resulted in significant deformation and compression of the RA (67 mL). In this extreme example observed in our series, both atria demonstrate extensive regions of low voltage (red) associated with regions of scar (grey) and fractionated signals (FS, pink tags). (*B*) Electroanatomic bipolar voltage map of a patient with MS (left) and a representative control (right). Both atria are oriented in the posterior-anterior projection and are of similar scale. The color scale is identical in both images with red representing low voltage areas ($\leq$0.5 mV) and purple being voltages $\geq$5 mV. The patient with MS (left image; LA 120 mL, RA 58 mL) has much larger atria that the control patient (LA 80 mL, RA 100 mL). In addition to having greater regions of low voltage (red), the patient with MS has regions of spontaneous scar (grey), and evidence of conduction abnormalities in the form of fractionated signals (FS, pink tags) and double potentials (DP, blue tags).

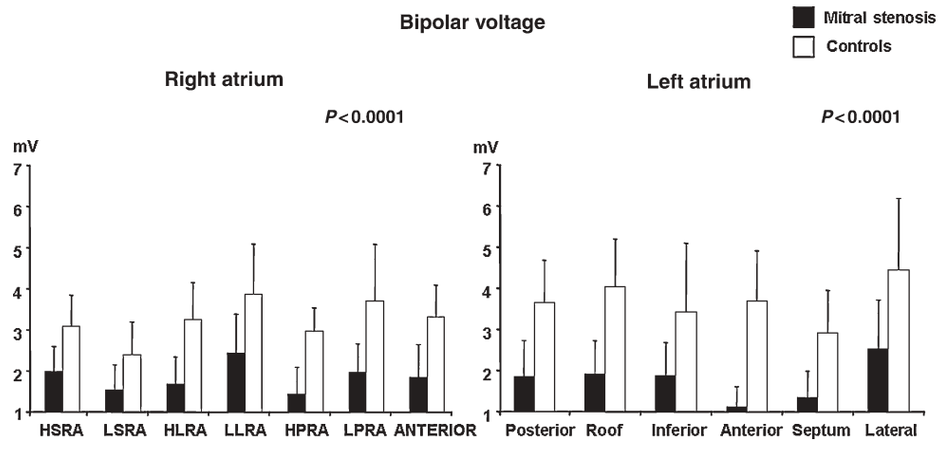

Figure 5 Regional differences in bipolar voltage between patients with mitral stenosis and controls for the right atria (left) and the left atria (right). Each region is as described in the text. Mixed effect group *P*-value for left atria and right atria are shown.

Atrial remodelling in conditions predisposed to atrial fibrillation

Wijffels *et al.* elegantly described the concept of atrial electrical remodelling in a study of AF in the conscious goat, demonstrating a fall in ERP and resultant decrease in atrial wavelength.[10] These seminal observations incriminated the decrease in ERP as an important factor promoting the maintenance of AF. However, studies evaluating the underlying substrate predisposing to AF have consistently demonstrated 'atrial remodelling of a different sort'.

Li *et al.* evaluated the effects on atrial remodelling in a canine model of congestive heart failure.[11] This study demonstrated no

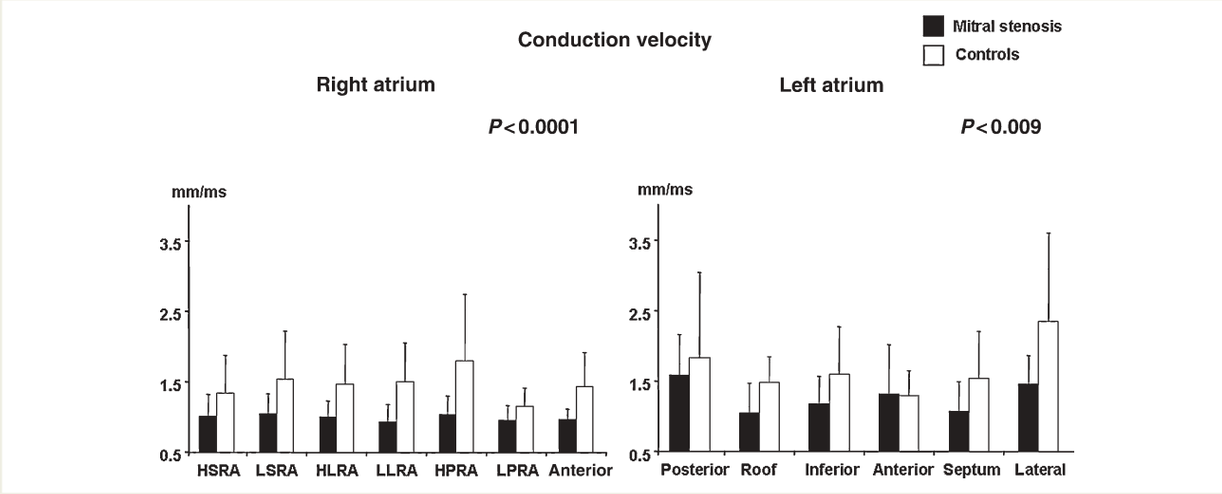

Figure 6 Regional differences in conduction velocity between patients with mitral stenosis and controls for the right atria (left) and the left atria (right). Each region is as described in the text. Significant differences are seen between patients with mitral stenosis and controls. Mixed effect group *P*-value for left atria and right atria are shown.

change in ERP at longer CLs, however, there was a significant increase in ERP at shorter CLs associated with an increase in the heterogeneity of conduction and marked interstitial fibrosis. As a result of these abnormalities in conduction and atrial structure, these animals demonstrated a significant increase in the duration of AF despite the increase in ERP. Verheule *et al.* have presented similar findings in a canine model of mitral regurgitation.[12] These investigators also observed an increase in ERP but a propensity for AF was presumed to be due to the observed abnormalities in conduction and profound structural remodelling.[12] Boyden *et al.* studied 23 dogs with spontaneous mitral valve fibrosis and left atrial enlargement (13 with intermittent and 10 with chronic AF).[13] These animals demonstrated no difference in the action potential duration, but it was noted that there were reduced numbers of muscle cell layers and an unusually large amount of connective tissue between greatly hypertrophied cells. All these studies have provided evidence arguing that the predominant contributor to the substrate for AF may be the structural abnormalities rather than the changes in ERP.

Clinical studies of the AF substrate have also demonstrated similar observations. Morton *et al.* studied the RA substrate in patients with atrial septal defects and observed prolonged ERPs and delayed conduction across the CT compared with controls.[14] Similarly, evaluation of the RA substrate in patients with congestive heart failure and sinus node disease have demonstrated prolonged ERPs and conduction times, and conduction delay at the CT associated with areas of low bipolar voltage and electrical silence or scar.[6,15] Recent studies in patients with AF undergoing ablation have also suggested the presence of areas of low voltage and scar, and have implicated this substrate as a marker of a worse outcome after a strategy of PV isolation alone.[16,17]

The present study is the only one to date that has evaluated the abnormalities in both the LA and RA in any clinical substrate predisposing to AF. In these patients with MS, we have observed no change or an increase in ERP in both the LA and RA, widespread and site-specific conduction delay which was observed in both atria, and structural change in the form of LA dilatation, evidence of loss of atrial myocardium and areas of electrical scar. Interestingly, despite a lack of difference in RA volume, patients with MS demonstrated a significant change in RA electroanatomic parameters. There are several potential mechanisms whereby the RA may manifest abnormalities in patients with MS: (i) direct injury as a result of rheumatic carditis; (ii) pulmonary hypertension with resultant chronic RA stretch; and (iii) potential neuro-hormonal factors that may affect both atria. Regardless of the exact mechanism, these patients with MS more frequently developed AF.

Prior studies on atrial remodelling in mitral stenosis

Fan *et al.* performed electrophysiological evaluation of the RA in 31 patients with MS at the time of PBMC.[18] Of these, 19 were in chronic AF and 12 in sinus rhythm at the time of the procedure. Following cardioversion of AF, these patients were found to demonstrate significantly shorter ERPs, sinus node dysfunction, and no significant difference in atrial conduction delay to extrastimuli compared with patients in sinus rhythm. At repeat study 3 months following PBMC, the ERPs had increased significantly compared with those who were in sinus rhythm. Soylu *et al.* evaluated the RA ERPs before and after PBMC in 25 patients with MS in sinus rhythm.[19] This study observed an acute increase in ERP immediately after PBMC. However, neither of these studies included a normal control group to determine the effects of MS independent of the effects of the arrhythmia itself or provided LA data. With the exception of these two studies, there has been no evaluation of the electrophysiological properties of the atrium in patients with MS.

Atrial structural changes in mitral stenosis

Structural change and its electrophysiological consequences are emerging as important determinants of atrial arrhythmias.[20,21] While these changes may be a consequence of atrial arrhythmias,[22] they may also occur as a result of a primary structural abnormality. Changes in cellular coupling due to interstitial fibrosis may result in spatial non-uniformity of propagation that can contribute to local conduction block and re-entry even in small regions of atrial tissue.[23]

In rheumatic MS a number of factors could result in structural abnormalities. It may be expected that in patients with RHD the primary disease process could potentially have a direct myocardial effect and that the mechanical consequences of the valvular disease may contribute to forming the substrate for AF. Several studies have documented the occurrence of ultrastructural changes resulting in fibrosis in the atria of patients with rheumatic MS.[24,25] A pathognomonic feature of rheumatic carditis is the Aschoff bodies; areas of fibrinoid necrosis surrounded by inflammatory cells.[26] Such inflammatory tissue can arise during the acute episode of carditis and remain immunologically active for years. They have been associated with the local release of a variety of cytokines, including many that are implicated in fibrogenesis.[27] Several other immunoactive cytokines have also been observed to be increased in plasma in patients with RHD.[28] In addition, recent studies have suggested remodelling of the matrix metalloproteinases as a result of mitral valve disease.[29]

In the present study, in patients with MS, both the LA and RA demonstrated significant reduction of bipolar voltage and some had evidence of areas of electrical scar. Although the reduction in voltage was observed in most regions, the distribution of areas of electrical silence was patchy, perhaps implicating a differential effect of stretch or the primary disease process on the atria. These changes were associated with the electrograms demonstrating DP and FS that result in inhomogeneous conduction, a necessary prerequisite for reentry. The presence of such extensive structural change may suggest that in patients with RHD, the mechanism initiating and maintaining AF could be diffusely located and different to that with lone AF.[30]

Study limitations

While the abnormalities observed in this study may constitute the substrate predisposing to AF, the development of clinical AF is complex and depends not only on substrate but also on other factors such as triggers and initiators that were not addressed by this study.

Conclusion

This study demonstrates that patients with rheumatic MS have significant bi-atrial remodelling characterized by atrial enlargement, loss of myocardium, and areas of electrical scarring associated with widespread and site-specific conduction abnormalities and no change or increased refractoriness. These abnormalities were associated with a heightened vulnerability for AF and may in part be responsible for the propensity for AF in patients with MS.

Acknowledgements

The authors acknowledge the statistical assistance received from Dr Anthony G. Brooks, Ph.D. and Mr Thomas Sullivan B.Ma.Comp.Sci. (Hons.), from the University of Adelaide.

Conflict of interest: P.S. reports having served on the advisory board of and having received lecture fees and research funding from Biosense-Webster, Bard Electrophysiology, St Jude Medical, and Medtronic.

Funding

B.J. is supported by the Biosense-Webster Electrophysiology Scholarship from the University of Adelaide. M.K.S. is supported by the National Heart Foundation of New Zealand and the Dawes Scholarship from the Royal Adelaide Hospital. L.M. is supported by the Peter Doherty Fellowship, National Health and Medical Research Council of Australia. P.S. is supported by the National Heart Foundation of Australia.

References

1. Agarwal BL. Rheumatic heart disease unabated in developing countries. *Lancet* 1981;**2**:910–911.
2. Carapetis JR, McDonald M, Wilson NJ. Acute rheumatic fever. *Lancet* 2005;**366**:155–168.
3. Benjamin EJ, Levy D, Vaziri SM, D'Agostino RB, Belanger AJ, Wolf PA. Independent risk factors for atrial fibrillation in a population-based cohort. The Framingham Heart Study. *JAMA* 1994;**271**:840–844.
4. Selzer A, Cohn KE. Natural history of mitral stenosis: a review. *Circulation* 1972;**45**:878–890.
5. Wolf PA, Dawber TR, Thomas HE Jr, Kannel WB. Epidemiologic assessment of chronic atrial fibrillation and risk of stroke: the Framingham study. *Neurology* 1978;**28**:973–977.
6. Sanders P, Morton JB, Davidson NC, Spence SJ, Vohra JK, Sparks PB, Kalman JM. Electrical remodeling of the atria in congestive heart failure: electrophysiological and electroanatomic mapping in humans. *Circulation* 2003;**108**:1461–1469.
7. Joseph G, Chandy S, George P, George O, John B, Jose V, Pati P. Evaluation of a simplified transseptal mitral valvuloplasty technique using over-the-wire single balloons and complementary femoral and jugular venous approaches in 1,407 consecutive patients. *J Invasive Cardiol* 2005;**17**:132–138.
8. Gepstein L, Hayam G, Ben Haim SA. A novel method for nonfluoroscopic catheter-based electroanatomical mapping of the heart. In vitro and in vivo accuracy results. *Circulation* 1997;**95**:1611–1622.
9. Kuklik P, Szumowski L, Zebrowski JJ, Walczak F. The reconstruction and analysis of the interior surface of the heart chamber from a set of points. *Physiol Meas* 2004;**25**:617–627.
10. Wijffels MC, Kirchhof CJ, Dorland R, Allessie MA. Atrial fibrillation begets atrial fibrillation. A study in awake chronically instrumented goats. *Circulation* 1995;**92**:1954–1968.
11. Li D, Fareh S, Leung TK, Nattel S. Promotion of atrial fibrillation by heart failure in dogs: atrial remodeling of a different sort. *Circulation* 1999;**100**:87–95.
12. Verheule S, Wilson E, Everett T, Shanbhag S, Golden C, Olgin J. Alterations in atrial electrophysiology and tissue structure in a canine model of chronic atrial dilatation due to mitral regurgitation. *Circulation* 2003;**107**:2615–2622.
13. Boyden PA, Tilley LP, Pham TD, Liu SK, Fenoglic JJ Jr, Wit AL. Effects of left atrial enlargement on atrial transmembrane potentials and structure in dogs with mitral valve fibrosis. *Am J Cardiol* 1982;**49**:1896–1908.
14. Morton JB, Sanders P, Vohra JK, Sparks PB, Morgan JG, Spence SJ, Grigg LE, Kalman JM. Effect of chronic right atrial stretch on atrial electrical remodeling in patients with an atrial septal defect. *Circulation* 2003;**107**:1775–1782.
15. Sanders P, Morton JB, Kistler PM, Spence SJ, Davidson NC, Hussin A, Vohra JK, Sparks PB, Kalman JM. Electrophysiological and electroanatomic characterization of the atria in sinus node disease: evidence of diffuse atrial remodeling. *Circulation* 2004;**109**:1514–1522.
16. Marcus GM, Yang Y, Varosy PD, Ordovas K, Tseng ZH, Badhwar N, Lee BK, Lee RJ, Scheinman MM, Olgin JE. Regional left atrial voltage in patients with atrial fibrillation. *Heart Rhythm* 2007;**4**:138–144.
17. Verma A, Wazni OM, Marrouche NF, Martin DO, Kilicaslan F, Minor S, Schweikert RA, Saliba W, Cummings J, Burkhardt JD, Bhargava M, Belden WA, Abdul-Karim A, Natale A. Pre-existent left atrial scarring in patients undergoing pulmonary vein antrum isolation: an independent predictor of procedural failure. *J Am Coll Cardiol* 2005;**45**:285–292.

18. Fan K, Lee KL, Chow WH, Chau E, Lau CP. Internal cardioversion of chronic atrial fibrillation during percutaneous mitral commissurotomy: insight into reversal of chronic stretch-induced atrial remodeling. *Circulation* 2002;**105**:2746–2752.
19. Soylu M, Demir AD, Ozdemir O, Topaloglu S, Aras D, Duru E, Sasmaz A, Korkmaz S. Evaluation of atrial refractoriness immediately after percutaneous mitral balloon commissurotomy in patients with mitral stenosis and sinus rhythm. *Am Heart J* 2004;**147**:741–745.
20. Jais P, Shah DC, Haissaguerre M, Hocini M, Peng JT, Takahashi A, Garrigue S, Le MP, Clementy J. Mapping and ablation of left atrial flutters. *Circulation* 2000; **101**:2928–2934.
21. Kall JG, Rubenstein DS, Kopp DE, Burke MC, Verdino RJ, Lin AC, Johnson CT, Cooke PA, Wang ZG, Fumo M, Wilber DJ. Atypical atrial flutter originating in the right atrial free wall. *Circulation* 2000;**101**:270–279.
22. Ausma J, Wijffels M, Thone F, Wouters L, Allessie M, Borgers M. Structural changes of atrial myocardium due to sustained atrial fibrillation in the goat. *Circulation* 1997;**96**:3157–3163.
23. Spach MS, Dolber PC. Relating extracellular potentials and their derivatives to anisotropic propagation at a microscopic level in human cardiac muscle. Evidence for electrical uncoupling of side-to-side fiber connections with increasing age. *Circ Res* 1986;**58**:356–371.
24. Thiedemann KU, Ferrans VJ. Left atrial ultrastructure in mitral valvular disease. *Am J Pathol* 1977;**89**:575–604.
25. Pham TD, Fenoglio JJ Jr. Right atrial ultrastructural in chronic rheumatic heart disease. *Int J Cardiol* 1982;**1**:289–304.
26. Ruebner BH, Boitnott JK. The frequency of Aschoff bodies in atrial appendages of patients with mitral stenosis. Relationship to age, atrial thrombosis, and season. *Circulation* 1961;**23**:550–561.
27. Fraser WJ, Haffejee Z, Jankelow D, Wadee A, Cooper K. Rheumatic Aschoff nodules revisited. II: Cytokine expression corroborates recently proposed sequential stages. *Histopathology* 1997;**31**:460–464.
28. Keiji Y, Uichi I, Hideaki M, Hideyuki F, Hiromichi S, Kazuyuki S. Endothelin production in pulmonary circulation of patients with mitral stenosis. *Circulation* 1994;**89**:2093–2098.
29. Anne W, Willems R, Roskams T, Sergeant P, Herijgers P, Holemans P, Ector H, Heidbuchel H. Matrix metalloproteinases and atrial remodeling in patients with mitral valve disease and atrial fibrillation. *Cardiovasc Res* 2005;**67**:655–666.
30. Nair M, Shah P, Batra R, Kumar M, Mohan J, Kaul U, Arora R. Chronic atrial fibrillation in patients with rheumatic heart disease: mapping and radiofrequency ablation of flutter circuits seen at initiation after cardioversion. *Circulation* 2001; **104**:802–809.